Novel Staggered Resonator Array Superconducting 2.3-GHz Bandpass Filter

George L Matthaei, *Life Fellow, IEEE,* and Gregory L. Hey-Shipton, *Member, IEEE*

***Abstract*—A novel stripline bandpass filter structure is presented which consists of a parallel array of equally spaced half-wavelength resonators. Couplings are controlled by introducing a small amount of stagger in the positions of the resonators. A very compact narrowband superconducting filter of this type was fabricated with excellent results. The design theory, computed and measured performance, and manner of construction are discussed.**

I. Introduction

THE novel stripline filter structure to be discussed has compactness and simplicity that make it very attractive for high-temperature superconducting filter applications, but these same properties also make it attractive for use in conventional filter applications. It gains its compactness from the fact that even for narrowband filters, all of its resonators can be closely packed together in a parallel array as shown in Fig. 1. It gains simplicity from the fact that no short-circuit connections are required so the structure is quite compatible with planar fabrication techniques.

By using high-temperature superconducting (HTS) films to construct this filter, very narrow bandwidths can be achieved with very low loss in a quite compact size. Although the design approach herein is also applicable to filters using normal conductors, the exceptionally high quality factors achievable with HTS films make the fabrication of an HTS filter for narrow bandwidths especially attractive. Such a filter has a performance that rivals that of waveguide, but in a very small size. Traditional end-coupled stripline filters have also been constructed using HTS films [1], but they rely on an entirely different coupling structure and result in relatively long filters. At the 2.3-GHz center frequency of the filter discussed herein, the resonators would be quite long, and a traditional end-coupled filter would be difficult to realize on a single HTS wafer.

Manuscript received March 22, 1993, revised June 14, 1993.

G. L. Matthaei is with Superconductor Technologies Inc., Santa Barbara, CA, and the Department of Electrical and Computer Engineering, University of California, Santa Barbara, CA 93106.

G. L. Hey-Shipton is with Superconductor Technologies Inc., Santa Barbara, CA 93111-2310.

IEEE Log Number 9212997.

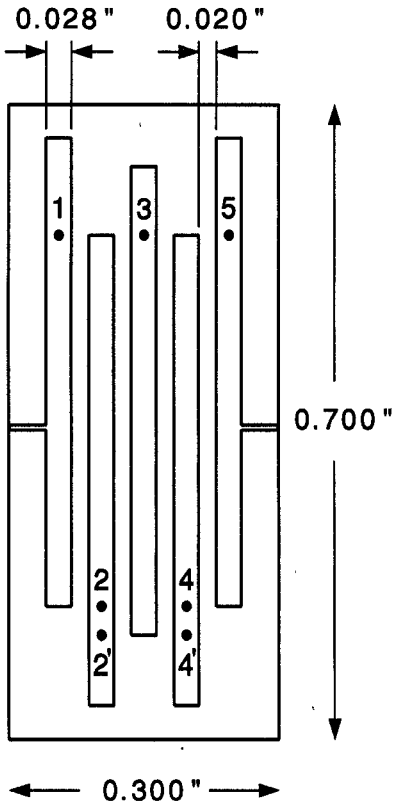

Fig. 1. A 5-resonator array bandpass filter.

II. Electrical Design

The type of filter under discussion consists of a parallel-array of half-wavelength resonators as shown in Fig. 1. The reader will note that the resonators are somewhat staggered in their relationships to their neighbors. It can be shown that if this type of filter is realized in stripline (which has equal even- and odd-mode wave velocities for coupled lines), and if these resonators are all positioned so that their top and bottom ends all fall on straight lines, this structure will have no passband at all, even if the resonators are very closely spaced. However, as we stagger each resonator with respect to its neighbors, coupling between the resonators is introduced and the structure has a passband. The more the resonators are staggered, the more coupling will result. Our point of view for the design of the narrowband HTS filter under discussion was to use quite closely spaced lines for compactness, with all of the coupled lines of the same width, and all of the spac-

0018-9480/93$03.00 © 1993 IEEE

ing between lines the same. Then the amount of stagger between lines provided the degree of freedom for fixing the resonator couplings.

The design point of view utilized is similar to that used by Dishal [2]. The method can be understood using Fig. 2 which shows a bandpass prototype for the filter. The prototype involves shunt resonators separated by admittance inverters, the parameters of which can be obtained from a low-pass prototype plus the desired bandwidth [3, Sec. 8.02]. To examine the coupling coefficient between two resonators, we can perform the experiment suggested in Fig. 3. There, resonator $k-1$ has been shorted, which reflects an open circuit to the left side of resonator k, while resonator $k+2$ has also be shorted, which reflects an open circuit to the right side of resonator $k+1$. Then the coupling between resonators k and $k+1$ can be examined with the effects of all other resonators removed. In Fig. 1, node points analogous to the numbered nodes in Fig. 2 are marked. These are chosen at the ends of regions of parallel coupling, and the nodal admittance at these points looks like that of a shunt tuned circuit. Because of the differences in amount of overlap between resonators, the node locations for exploring coupling are, for example, different on resonator 2 when considering coupling between resonators 1 and 2 than when considering coupling between 2 and 3.

Fig. 4 illustrates how we apply the principles of Figs. 2 and 3 to an array of resonators as in Fig. 1. In Fig. 4, the operation of resonators k and $k+1$ can be examined while resonators $k-1$ and $k+2$ are shorted out. To achieve this effect, the impedances Zoe' and Zoo' are the even- and odd-mode impedances of lies k and $k+1$ *operated in the presence of lines* $k-1$ *and* $k+2$ *at zero potential*. The calculation of these impedances will be discussed later in this section. The dimensions of the uncoupled line sections Z_k and Z_{k+1} are slightly different from those for the coupled part of the lines. We make these uncoupled line sections have an impedance equal to that of the coupled part of the line when both adjacent lines are grounded. Relating the parameters in Fig. 4 to those in Fig. 3, it can be shown that the resonator susceptances seen at nodes k and $k+1$ are

$$B_k = B_{k+1} = \frac{-(Zoe' + Zoo')\sin(2\theta)}{[(Zoe' + Zoo')^2 \sin^2\theta - 4Zoe'Zoo']} + \frac{\tan(a\theta)}{Z_k} \tag{1}$$

where $\theta = \omega L/v$ is the electrical length of the parallel-coupled region; v is the wave velocity in the stripline medium; and a, Z_k, and Z_{k+1} are as defined in Fig. 4. In order to achieve resonance at the specified midband frequency ω_o, we enforce the relation

$$a = \frac{1}{\theta_o}\tan^{-1}\left|\frac{Z_k(Zoe' + Zoo')\sin(2\theta_o)}{[(Zoe' + Zoo')^2 \sin^2\theta_o - 4Zoe'Zoo']}\right| \tag{2}$$

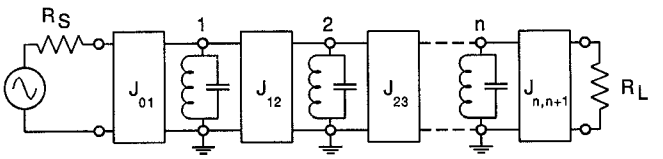

Fig. 2. Prototype for a resonator array bandpass filter.

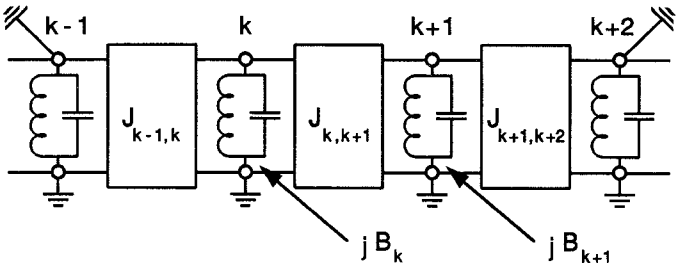

Fig. 3. Circuit arrangement for observing the coupling between resonators k and $k+1$.

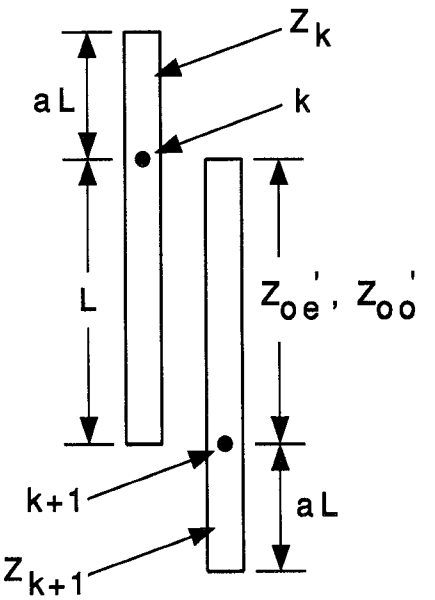

Fig. 4. A coupled-transmission line equivalent to the circuit in Fig. 3. The definition of Zoe' and Zoo' is explained in the text.

where $\theta_o = \omega_o L/v$. The admittance parameter $J_{k,k+1}$ for the inverter between the resonators is found to be

$$J_{k,k+1} = \left|\frac{2(Zoe' - Zoo')\sin\theta_o}{[(Zoe' + Zoo')^2 \sin^2\theta_o - 4Zoe'Zoo']}\right|. \tag{3}$$

To get the coupling coefficient $k_{k,k+1}$ between resonators, we first compute the resonator slope parameters

$$b_k = b_{k+1} = \frac{\theta_o}{2}\frac{dB}{d\theta}\bigg|_{\theta=\theta_o} \tag{4}$$

which we compute numerically from (1) and (2). Then the coupling coefficient is

$$k_{k,k+1} = \frac{J_{k,k+1}}{\sqrt{b_k b_{k,k+1}}}. \tag{5}$$

Using the above information, the interior part of the filter is designed by first determining the resonator coupling coefficients needed for the desired design [3], and then computing some values of coupling coefficient versus resonator overlap electrical length θ_o from which the appropriate overlaps for the needed couplings can be determined.

The coupling between the end resonators and the terminations is fixed by the tap locations in Fig. 1 which control the external Q's of the end resonators. Fig. 5 shows how resonator 1 is modeled for this purpose, where the impedance Z_1' is the impedance of resonator 1 in the presence of resonator 2 grounded. The susceptance of this resonator as seen at the tap connection point is given by

$$B_1 = \frac{[\tan(\{1 - c\}\phi) + \tan(c\phi)]}{Z_1'} \tag{6}$$

where c fixes the tap point and ϕ is equal to π at resonance. After determining the resonator susceptance slope parameter b_1, the external Q of the resonator is found to be

$$(Q_{ex})_1 = \frac{b_1}{Y_o} = \frac{\pi}{2}\frac{Z_o}{Z_1'}[(1 - c)\sec^2\{(1 - c)\pi\} + c\sec^2(c\pi)]. \tag{7}$$

The tap position at the other end of the filter can be computed in a similar manner although this will usually be unnecessary because in most cases the desired design is symmetrical.

Let us now consider means for computing the even- and odd-mode impedances of two coupled lines embedded between two grounded lines, as is required for the impedances *Zoo'* and *Zoe'* in Fig. 4 and the design procedure described above. Using the capacitance decomposition procedure described below, the necessary impedance values can be determined with the aid of any program that can compute the characteristic impedance of a single stripline and the even- and odd-mode impedances of a pair of symmetrical coupled striplines. In order to simplify the drawings for explaining the decomposition of the line capacitances into components, the drawings will be made in terms of hypothetical microstrip lines in a homogeneous dielectric. The equations and concepts for analogous stripline cases are the same.

Since the dielectric in the structures in Fig. 6 is assumed to be homogeneous, for TEM-mode propagation, the characteristic impedance of the single line at (a) can be computed by

$$Zos = \frac{1}{v(2C_f)}. \tag{8}$$

Here v is again the wave velocity and C_f is half the capacitance per unit length between the line and the ground plane. Here we use the subscript f because this line has freely fringing fields at its sides. In Fig. 6(b) is shown the case of two coupled lines each of which has the same width as the line at (a). In this case, the capacitance to ground of the inner half of each line is somewhat suppressed due to the presence of the adjacent line, and this capacitance is labeled C_s. In addition, there is coupling

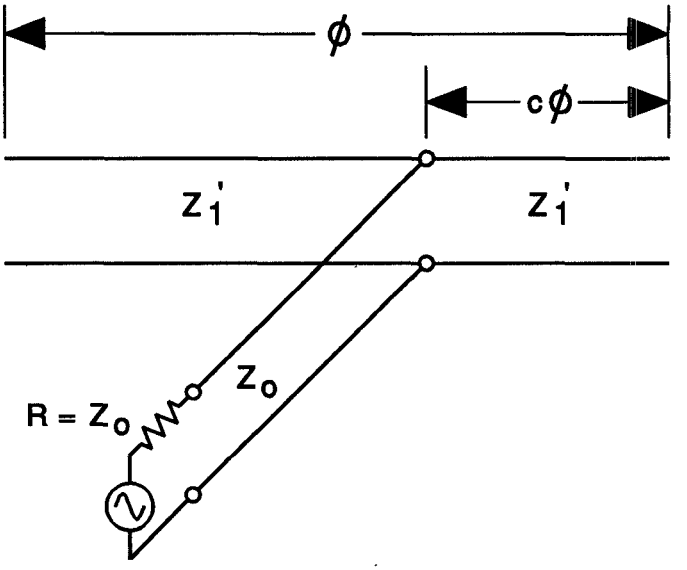

Fig. 5. Equivalent circuit for computing tap location for end resonators.

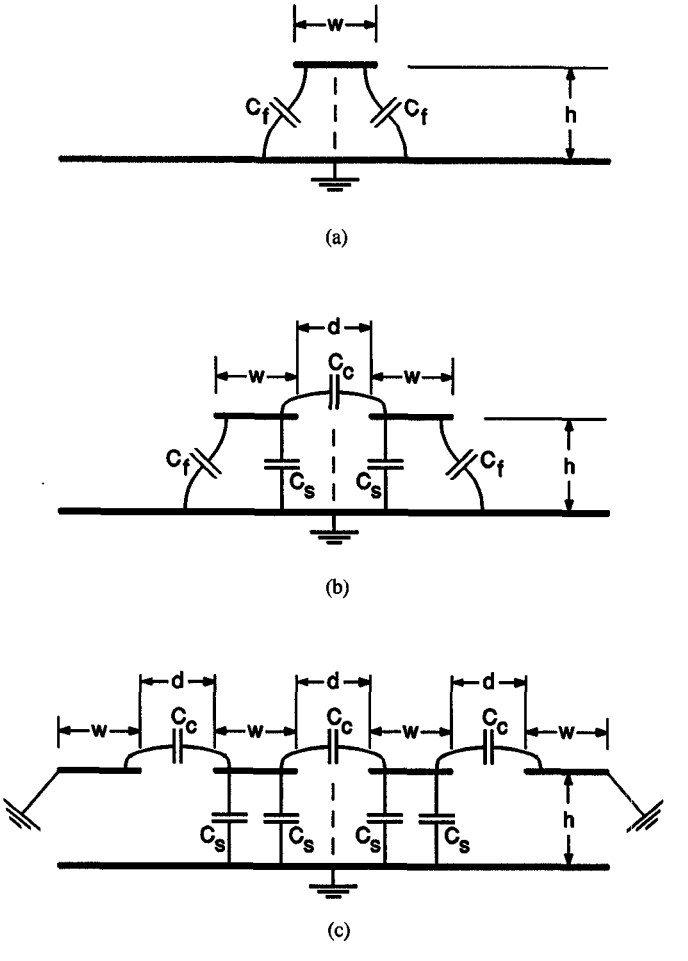

Fig. 6. Representation of the distributed capacitances associated with transmission lines in terms of component capacitances.

capacitance C_c between the two lines. In terms of these component capacitances, the even- and odd-mode impedances, respectively, of the coupled lines can be seen to be

$$Zoe = \frac{1}{v(C_s + C_f)} \tag{9}$$

$$Zoo = \frac{1}{v(C_s + C_f + 2C_c)}. \tag{10}$$

Using these equations, if the impedances *Zos*, *Zoe*, and *Zoo* are obtained for a single stripline and a corresponding pair of lines spaced d apart, by use of any of several commercial CAD programs, then C_f, C_s, and C_c can be solved for using the above equations.

Fig. 6(c) shows the transmission-line situation corresponding to the problem in Fig. 3 where it is desired to analyze the coupling between resonators k and $k + 1$, and it is necessary to ground resonators $k - 1$ and $k + 2$ in order to eliminate them from the analysis. The reader will note that the effect of adding the grounded lines on the far left and far right in Fig. 6(c) is that the fringing capacitances C_f in Fig. 6(b) are replaced by capacitances $(C_s + C_c)$ in Fig. 6(c). Therefore, in this case, the even- and odd-mode impedances become

$$Zoe' = \frac{1}{v(2C_s + C_c)} \tag{11}$$

and

$$Zoo' = \frac{1}{v(2C_s + 3C_c)}. \tag{12}$$

These are the impedances needed for use in the design equations (1)–(3). In the case of the coupling between an end resonator and its nearest neighbor, there is free fringing on the outer side of the end resonator, but the coupling analysis calls for a grounded resonator on the inner side of the adjacent resonator within the resonator array. To treat this, we simply used a resonator overlap L which was the average of the results obtained using the impedances in (9) and (10), and the results using (11) and (12).

With regard to the impedances to be used for the sections of line aL in Fig. 4 which are not coupled, note in Fig. 3 that if you wished to analyze the performance of resonator k by itself, you could do so by grounding the adjacent resonators $k - 1$ and $k + 1$. From this, we conclude that the fundamental impedance associated with resonator k is that of line k with the adjacent lines grounded. This impedance is

$$Z_k = \frac{1}{v(2C_s + 2C_c)}. \tag{13}$$

Thus, it is desired for the uncoupled portions of the resonators to also have this impedance. By use of a CAD program, the necessary strip width to achieve this impedance is readily determined. The uncoupled portion of each strip will, as a result, be slightly wider than the coupled portion. For the case of the end resonators as in Fig. 5, their impedance should be evaluated with the adjacent resonator grounded. Therefore, the impedance Z_1' for the resonator in Fig. 5 is given by

$$Z_1' = \frac{1}{v(C_c + C_s + C_f)}. \tag{14}$$

III. A Trial Design for Use with HTS

Using the methods outlined above, an HTS, 5-resonator filter was designed for a 2.62 percent bandwidth centered at 2.3 GHz with a 0.05-dB Chebyshev passband ripple. The design was worked out as described above, starting from a lumped-element low-pass prototype. The theoretical response of this design was computed using approximations (which are described in Section V) used in the Touchstone™ CAD program. Initially, the response showed a small amount of mistuning as evidenced by gradually varying ripple amplitudes across the passband. Increasing the lengths of the end resonators by 0.15 percent, and reducing the lengths of the adjacent resonators by 0.06 percent, gave near-perfect passband symmetry will all ripples 0.05 dB or slightly less. The computed passband width was 2.65 percent (as compared to the 2.62 percent design objective), and the center frequency was correct. Thus, the computed response of the design was highly accurate except for some small, resonator tuning errors. These small tuning corrections in the resonator lengths were incorporated into the final design along with corrections for the fringing fields at the ends of the strips.

The practical HTS realization of this filter required dealing with complications which need not be involved when this type of filter is used for more conventional applications. As in [1], the stripline structure was fabricated using two substrates, the top substrate having the upper ground plane on its top side, and the circuit pattern on its lower side, and the lower substrate having the circuit pattern on its top and a ground plane on the bottom, all conductors being thallium-barium-calcium-copper-oxide (TBCCO) HTS films. The circuit pattern was included on both substrates in order to avoid possible problems with a small air gap between substrates. The substrates used were lanthanum aluminate ($LaAlO_3$) and had a relative dielectric constant of about 24 which, along with the inherent compactness of this kind of filter, made the filter very small. The stripline filter was made from two 0.020-in-thick substrates, resulting in a stripline ground plane spacing of 0.040 in. The size of the upper substrate was 0.7×0.3 in, and the lower one 0.7×0.54 in. They were enclosed in a metal housing as described below.

The major problems with packaging this kind of HTS stripline circuit is due to the hard substrate material ($LaAlO_3$) upon which the films are fabricated. These hard substrates tend to create grounding and interface problems. Fig. 7 shows the technique adopted to solve the grounding and interface problems. The 50 Ω connecting line to the circuit pattern for the stripline filter on the lower substrate was extended to the edge of the substrate but

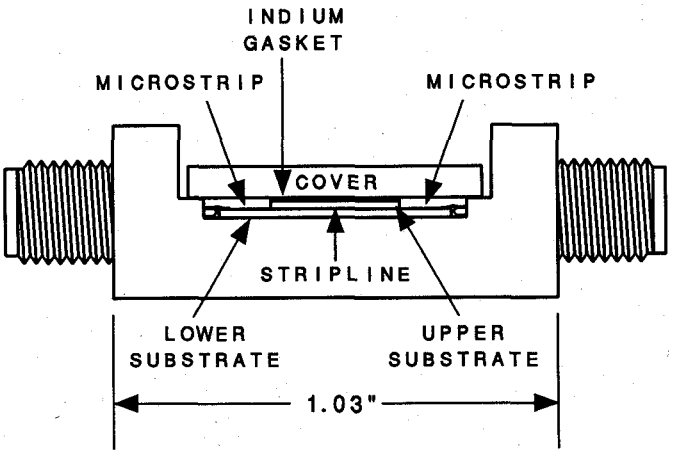

Fig. 7. Construction of the stripline filter.

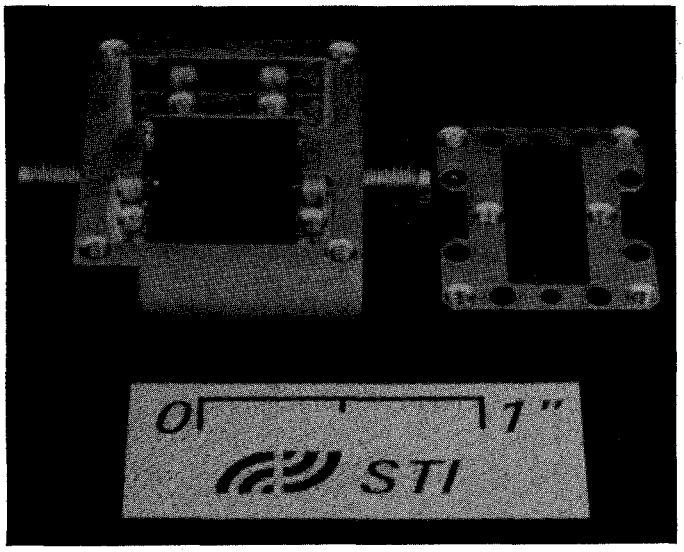

Fig. 8. Photograph of the 2.3-GHz stripline filter.

with the upper dielectric removed. Then the width of the line was increased to compensate for the air dielectric above the line. This created a sort of microstrip transmission line at each end of the filter that facilitated the bonding of gold ribbons from the ohmic gold contacts deposited on this line to the connector pins. However, the upper ground cover from the stripline section was extended over the microstrip-like line in order to provide a path with minimal discontinuities for the stripline ground currents to the housing. Fig. 8 shows a picture of a disassembled filter, with the smaller upper substrate on the inner cover and the lower substrate in the housing (the circuit patterns are difficult to see as the TBCCO HTS has a very dark color).

As stated earlier, the circuit pattern for the filter was included on both substrates due to the problems that are created by a possible small air gap between the two substrates. Tests conducted on filters manufactured with just single circuit patterns showed greatly deteriorated performance. The circuit pattern on the upper and lower substrates needs to be carefully aligned. This was accomplished by the use of cross hair targets etched into the circuit side of the upper substrate with a corresponding negative image etched into the circuit side of the lower substrate. These were located at all four corners of the upper substrate for greatest accuracy, and in order to allow light to enter through the edges of the substrate, thereby allowing alignment using standard laboratory microscopes and lighting.

IV. Performance of the Filter

The solid line in Fig. 9 shows the measured insertion loss of this filter when operated at 77K, while the dashed line shows the computed response discussed in Section III, which was obtained by means explained in Section V. Although accurate measurement of very small attenuation in a cryogenic environment is quite difficult, the measured centerband insertion loss appeared to be around 0.1 dB (the calibration was done using a coaxial barrel connector which approximates the loss in the connectors). It is not certain what resonator unloaded Q's were realized with this filter, but recent measurements made at 8.2 GHz with a single test resonator, similar to those used in this filter, showed an unloaded Q in excess of 20 000. The shape of the measured passband is very symmetric, which indicates that the resonant frequencies of the resonators are all synchronous. The ripples in the measured passband insertion loss were greater than the 0.05-dB design objective. This may have resulted from the fact that no attempt was made in the design process to try to compensate for the junction effects at the tap points on the resonators at the ends. A small readjustment of the tap-point locations could have compensated for this. It is seen that the measured response is somewhat wider than the design objective and centered a little high. This appears to be due to some discrepancy between the actual physical parameters (i.e., capacitances and wave velocity) and those used in the theoretical model, since in terms of the parameters used in the theoretical model, the response was computed to be extremely accurate. However, for most practical purposes the measured response in Fig. 9 is quite good. The response was obtained without the use of any tuning.

V. Derivation of (1)–(3), and Computation of the Circuit Response

Equations (1)–(3) are used along with (4) and (5) to calculate the coupling coefficient between pairs of resonators as in Fig. 4 for a given amount of resonator overlap L. In order to simplify the analysis, we will first remove the uncoupled sections aL and deal with the simpler circuit in Fig. 10. Using methods such as those in [4], the open-circuit impedances with reference to ports a and b in Fig. 10 are seen to be

$$z_{aa} = z_{bb} = -j(Zoe' + Zoo') \cot(\theta)/2 \qquad (15)$$

and

$$z_{ab} = z_{ba} = -j(Zoe' - Zoo') \csc(\theta)/2. \qquad (16)$$

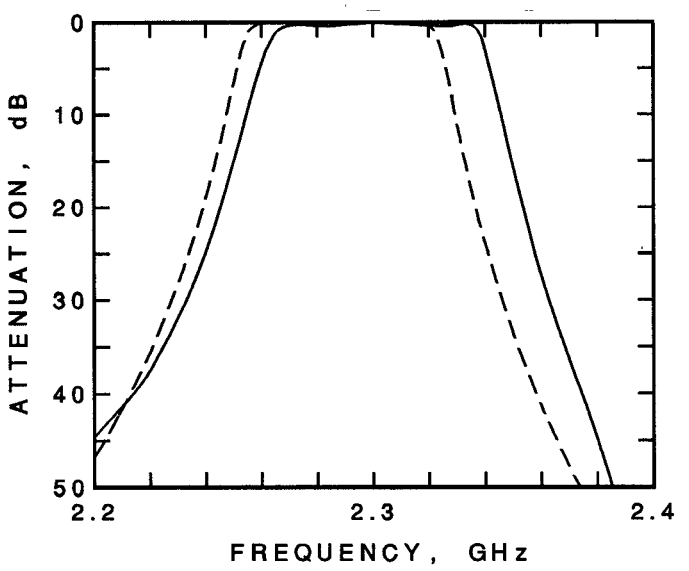

Fig. 9. The solid line shows the measured response, and the dashed line shows the computed response of the 2.3-GHz stripline filter.

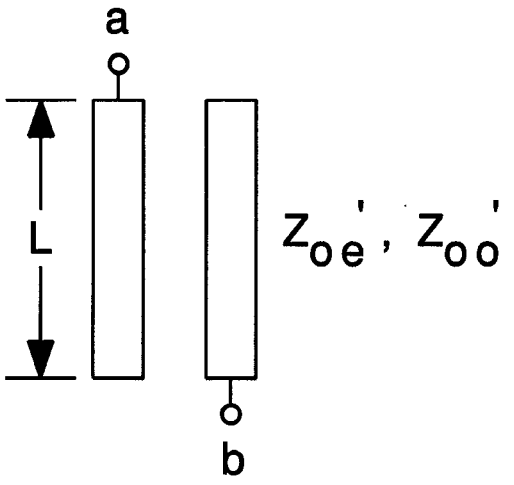

Fig. 10. The circuit in Fig. 4 with the uncoupled line sections aL removed.

Since the resonances exhibited at nodes k and $k+1$ in Fig. 4 will be of the shunt type as suggested in Fig. 3, and since we will want to be adding the line sections Z_k and $Z_{k,k+1}$ in Fig. 4 in shunt at terminals a and b in Fig. 10, it will be most convenient to deal with the circuit in Fig. 10 on the admittance basis. Inverting the open-circuit-impedance matrix gives the corresponding short-circuit admittances which are

$$y_{aa} = y_{bb} = \frac{-j(Zoe' + Zoo')\sin(2\theta)}{[(Zoe' + Zoo')^2 \sin^2(\theta) - 4Zoo'\,Zoe']} \tag{17}$$

$$y_{ab} = y_{ba} = \frac{j2(Zoe' - Zoo')\sin(\theta)}{[(Zoe' + Zoo')^2 \sin^2(\theta) - 4Zoo'\,Zoe']}. \tag{18}$$

Now the pie equivalent circuit in Fig. 11(a) for the circuit in Fig. 10 can be obtained from the short-circuit admittances by

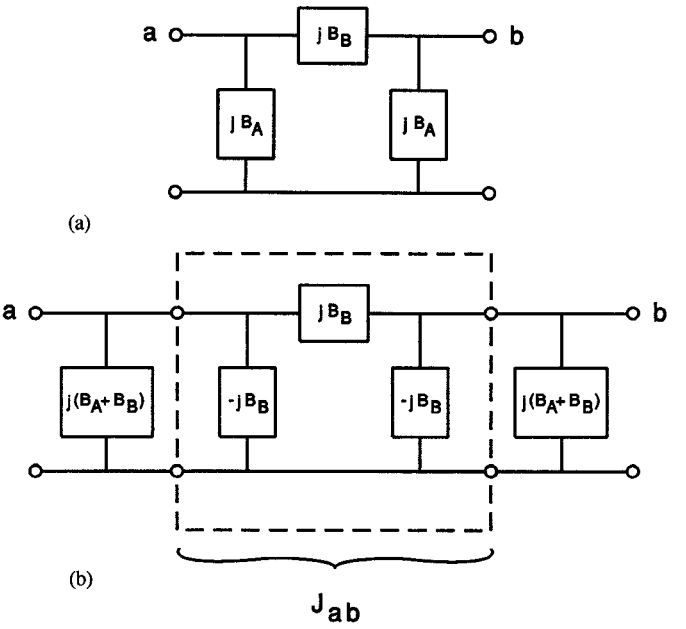

Fig. 11. Some pi equivalent circuits for the circuit in Fig. 10.

$$jB_A = y_{aa} = y_{ab}, \qquad jB_B = -y_{ab}. \tag{19}$$

The circuit in Fig. 11(b) is electrically the same as that in Fig. 11(a), but it has been altered by adding positive and negative shunt susceptances jB_2. It can be seen from [3, Sec. 8.03] that the pi network at the center of Fig. 11(b) comprises an admittance inverter with an inverter parameter of

$$J_{ab} = |B_B| \tag{20}$$

which gives (3). In order to obtain the total resonator susceptances, we must add the susceptances of the line sections of length aL in Fig. 4 to the terminals of the network in Fig. 10. This gives

$$jB_k = jB_{k+1} = jB_A + jB_B + j\frac{\tan(a\theta)}{Z_k} \tag{21}$$

which is (1). To get (2), (1) is set equal to zero and solved for a in order to establish the length that will give resonance.

Most microwave CAD programs will require the use of added approximations in order to analyze a circuit, such as that in Fig. 1, since they are only set up to compute the coupling between two parallel lines. We found that the scheme shown in Fig. 12 works quite well for stripline circuits where the coupling beyond nearest neighbors can be neglected.[1] Each resonator line is split into two parallel lines which are regarded as being totally independent up to their ends where they are connected together. The coupling between two lines separated by a coupling gap is accounted for entirely by the coupling between the *half lines* which are adjacent to that gap. In terms of the lines

[1]A reviewer of this paper called to the authors' attention that a similar approach was previously used in [5].

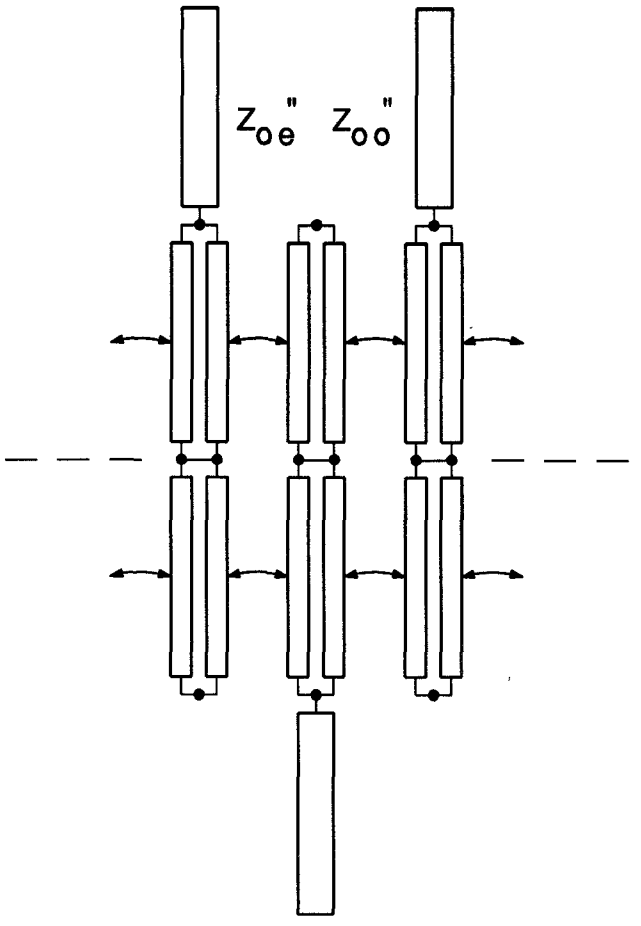

Fig. 12. The sketch above suggests how the circuit in Fig. 1. can be broken up in order to be analyzed with a conventional CAD program. The curved arrows indicate the coupling between adjacent half lines.

and notation used in Section II, the even- and odd-mode impedances for the coupled half lines are given by

$$Zoe'' = \frac{1}{vC_s}, \qquad Zoo'' = \frac{1}{v(C_s + 2C_c)} \tag{22}$$

In the case of the resonators at the ends of the array, the outer half lines do not have any coupling, so have only the single impedance

$$Z_f = \frac{1}{vC_f} \tag{23}$$

which includes the effect of the free-fringing fields at the outer edges of the strips. (This technique of representing a pair of coupled lines by two sets of halflines connected at their ends, with the coupling included only between the inner half lines, was first tested with a directional coupler and was found to give very little error.) Additional coupled and uncoupled half lines are needed to model the cases such as nodes 2 and 2′, and 4 and 4′ in Fig. 1, where the coupling lengths are different for the two half lines of a given strip. However, the principles as discussed above still apply. We used these approximations along with the Touchstone program for computing the frequency response.

Judging from how well the computed response agreed with the design specifications, it appears that the model using half lines in Fig. 12 is quite accurate if coupling beyond nearest neighbors can be neglected (as is usually true for stripline). In Fig. 12, each half-line section is somewhat less than a quarter-wavelength long in the frequency band of interest. We tried reducing the lengths of the half lines by one-half and doubling the number of half lines to see if this would changed the response. That had a negligible effect.

VI. Concluding Remarks

Stripline filter structures of the general form of that in Fig. 1 are seen to provide a very practical means for designing very compact filters, especially for narrowband applications. This type of structure can also be fabricated in microstrip, but that would not be desirable for high-Q HTS applications because radiation would seriously degrade the very high Q's of the resonators. However, for more conventional microstrip applications, where the small amount of radiation present is acceptable, microstrip structures of this type should be feasible for some applications. But the difference between the even- and odd-made velocities for the coupled microstrip lines introduces "forward coupling," and the design equations must be modified to include that effect. Shortly before this paper went to press, we generalized our design equations for that situation and found that even with no stagger in the resonators, there was far too much coupling for the narrowband application we had in mind. However, such microstrip structures might be useful for more wideband filters. A possible complication is that with closely spaced microstrip lines, it may be important to include coupling beyond nearest neighbors if high accuracy is required.

The upper stopband of our trial filter was degraded by waveguide mode activity within the filter housing. (The attenuation level was reduced to around the 30-dB level in regions where we would otherwise expect much more attenuation.) Since for the application we had in mind, this degradation was of no importance, we did not pursue this matter, and assumed such mode activity could be suppressed, if need be. As this paper goes to press, we had occasion to consider this matter further, and believe the degradation was due to weak coupling to a waveguide mode propagating from left to right in Fig. 1. The coupling to this mode is probably due to the structural asymmetry in the vertical direction in the microstrip regions next to the connectors (see Fig. 7). It may be that this mode activity can be suppressed by adding lossy material along the shorter sides of the housing (i.e., along the top and bottom edges in Fig. 1). However, we have not had an opportunity to try this.

References

[1] G. L. Matthaei and G. L. Hey-Shipton, "High-temperature superconductor 8.45-GHz bandpass filter for the deep space network," in *1993 MTT-S Int. Microwave Symp. Dig.*, Paper LL-2.

[2] M. Dishal, "Alignment and adjustment of synchronously tuned multiple-resonant-circuit filters," *Proc. IRE*, vol. 39, pp. 1448–1455, Nov. 1951.
[3] G. L. Matthaei, L. Young, and E. M. T. Jones, *Microwave Filters, Impedance-Matching Networks, and Coupling Structures*. Norwood, MA: Artech House, 1980.
[4] E. M. T. Jones and J. T. Bolljahn, "Coupled-strip transmission line filters and directional couplers," *IRE Trans. Microwave Theory Tech.*, vol. PGMTT-4, pp. 75–81, Apr. 1956.
[5] C. Denig, "Using microwave CAD programs to analyze microstrip interdigital filters," *Microwave J.*, vol. 26, pp. 147–152, Mar. 1989.

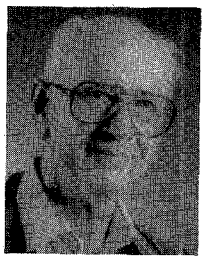

George L. Matthaei (F'65–LF'89) received the B.S. degree from the University of Washington in 1948, and the Ph.D. degree from Stanford University in 1952.

From 1951 to 1955 he was on the faculty of the University of California, Berkeley, where he was an Assistant Professor, and his specialty was network synthesis. From 1955 to 1958 he was engaged in system analysis and microwave component research at the Ramo-Wooldridge Corporation. From 1958 to 1964 he was at Stanford Research Institute where he was engaged in microwave device research and became Manager of the Electromagnetic Techniques Laboratory in 1962. In July 1964 he joined the Department of Electrical Engineering at the University of California, Santa Barbara, where he was a Professor and in July 1991 became a Professor Emeritus. Since September 1991 he has also been part time at Superconductor Technologies, Inc. He is the author of numerous papers, coauthor of the book *Microwave Filters, Impedance-Matching Networks and Coupling Structures*, and a contributor to several other books. His current interests are in the area of passive and active microwave and mm-wave circuits and, in particular, application of high-temperature superconductivity to such circuits.

Dr. Matthaei is a member of Tau Beta Pi, Sigma Xi, and Eta Kappa Nu. He was a winner of the 1961 Microwave Prize of the IEEE MTT Group. In 1984 he received an IEEE Centennial Medal, and in 1986 received the Microwave Career Award of the IEEE Microwave Theory and Techniques Society.

Gregory L. Hey-Shipton (M'82) received the Ph.D. degree from Leeds University, England, in 1978.

He was with Watkins-Johnson Company from 1978 to 1991, at several locations, finally as Department Manager of the Subsystems Product Engineering Department, in Palo Alto, CA. He joined Superconductor Technologies Inc. in Santa Barbara, CA, in June 1991 as the Engineering Manager, and was made Vice President of Engineering in March 1992.